Finite Element Modeling and Optimization of Tube-Shaped Ultrasonic Motors

P. Bouchilloux[*a], Serra Cagatay[b], Kenji Uchino[b], Burhanettin Koc[c]
[a]Adaptronics, Inc., 1223 Peoples Ave., Troy, NY 12180;
[b]International Center for Actuators and Transducers, Materials Research Laboratory, The Pennsylvania State University, University Park, PA, 16802;
[c]Kirikkale University, Department of Electrical and Electronics Engineering, Turkey.

ABSTRACT

Recent developments in ultrasonic motor design have demonstrated that small size tube-shaped motors could be fabricated at low cost. Motors with diameters between 15 and 2.5mm have been fabricated and tested. The performance evaluation of these motors is still in progress, but have already shown promising results: the smallest ones exhibit no-load speeds in the range of 70rad/s and blocked torques close to 0.9mN·m.

In this paper, we review the operating principle of these devices and several implementation examples. Then, we show how the finite element method (ATILA) can be used, in combination with genetic optimization procedures, to design tube-shaped motors in various dimensions and for different performance objectives. Several design examples are presented and discussed.

Keywords: ultrasonic motors, piezoelectric, finite element analysis, genetic optimization

1. INTRODUCTION

Piezoelectric ultrasonic motors display exceptional properties, such as high resolution and motion control, absence of parasitic magnetic fields, frictional locking at rest, and high thrust to weight ratio. These motors are good candidates for use in precision micromechanical systems. Medical applications such as, endoscopes and prosthetic devices could also benefit from miniature motors. Endoscopy techniques are replacing many surgical procedures. Instead of a critical surgery, a thin tube is inserted through a small slit and moved to the appropriate place in the body. Miniature motors would add additional functionality to such endoscopic procedures [1].

Miniaturization of piezoelectric motors can be accomplished if the structure and driving circuit of these motors are simplified so that they can be manufactured at low cost. One of the most suitable structures for miniaturization of piezoelectric motors is multi- (or mixed-) mode excitation type piezoelectric motor. Exciting at least two orthogonal resonance modes of the stator vibrator generates elliptical motion on the stator surface. According to the shape of the stator, these orthogonal resonance modes may generate longitudinal-torsional [2,3] radial-torsional [4], translational-flexural [5], longitudinal-flexural [6], or flexural-flexural motions. The stators of these types of motors may have some additional elastic part, which is called a vibration coupler or a concentrator. Single mode vibration on the piezoelectric element is converted into multi mode vibration at the tip of the concentrator. Either exciting two different electrode groups one at a time or tuning the driving frequency of the stator vibrator to a different orthogonal frequency pair controls the rotation or direction of the linear motion. If multi-vibrators are used, either the vibration or orientation of the vibrators needs to be orthogonal. In this type of motor, superimposing two orthogonal single mode vibrations with a phase shift generates elliptical motion.

The motor presented in this paper is a multi-mode-single-vibrator excitation type, which uses two orthogonal bending modes of a hollow cylinder. Since the structure and poling configuration of the active piezoelectric elements used in the

[*] pb@adaptronics.com; phone 518-266-1146; fax 518-266-1142; www.adaptronics.com

Report Documentation Page

Form Approved
OMB No. 0704-0188

1. REPORT DATE	2. REPORT TYPE	3. DATES COVERED
00 JUN 2003	**N/A**	**-**

4. TITLE AND SUBTITLE	5a. CONTRACT NUMBER
Finite Element Modeling and Optimization of Tube-Shaped Ultrasonic Motors	5b. GRANT NUMBER
	5c. PROGRAM ELEMENT NUMBER
6. AUTHOR(S)	5d. PROJECT NUMBER
	5e. TASK NUMBER
	5f. WORK UNIT NUMBER
7. PERFORMING ORGANIZATION NAME(S) AND ADDRESS(ES) **Adaptronics, Inc., 1223 Peoples Ave., Troy, NY 12180; International Center for Actuators and Transducers, Materials Research Laboratory, The Pennsylvania State University, University Park, PA, 16802; Kirikkale University, Department of Electrical and Electronics Engineering, Turkey.**	8. PERFORMING ORGANIZATION REPORT NUMBER
9. SPONSORING/MONITORING AGENCY NAME(S) AND ADDRESS(ES)	10. SPONSOR/MONITOR'S ACRONYM(S)
	11. SPONSOR/MONITOR'S REPORT NUMBER(S)

12. DISTRIBUTION/AVAILABILITY STATEMENT
Approved for public release, distribution unlimited

13. SUPPLEMENTARY NOTES
See also ADM001697, ARO-44924.1-EG-CF, International Conference on Intelligent Materials (5th) (Smart Systems & Nanotechnology)., The original document contains color images.

14. ABSTRACT

15. SUBJECT TERMS

16. SECURITY CLASSIFICATION OF:			17. LIMITATION OF ABSTRACT	18. NUMBER OF PAGES	19a. NAME OF RESPONSIBLE PERSON
a. REPORT	b. ABSTRACT	c. THIS PAGE			
unclassified	**unclassified**	**unclassified**	**UU**	**10**	

stator are simple, this motor structure is very suitable for miniaturization. Moreover, a single driving source can excite two bending modes at the same time, thus generate a wobble motion. This motor may find applications in the medical industry (endoscopes and prosthetic devices), mechatronics (miniature telerobotic), information devices (silent alarm) and horology.

Piezoelectric motors using bending vibrations of a square beam were first proposed by Williams and Brown in 1942. Their design included four piezoelectric rectangular plates bonded to the faces of a square elastic beam. A wobbling motion of this "stator" was generated at one end of the bar upon exciting piezoelectric elements by two voltage signals such as sine and cosine at a bending mode resonance frequency of the square beam. A rotor was then pressed against the stator's tip and a rotation was produced via frictional interaction between the contacting surfaces [7].

Even though the principle and the structure of the piezoelectric motor proposed by Williams *et al.* is similar to more modern piezoelectric motors [8,9,10], the original piezoelectric motor never became a commercial product due to the lack of high quality piezoelectric materials and high voltage-high frequency driving techniques.

2. STRUCTURE AND OPERATING PRINCIPLE

A square beam has two orthogonal bending modes whose resonance frequencies are equal to each other. The first bending mode frequencies in any direction for circular cylinders are also equal to each other. The stator of the motor presented in this study combines the circular and square cross-sections.

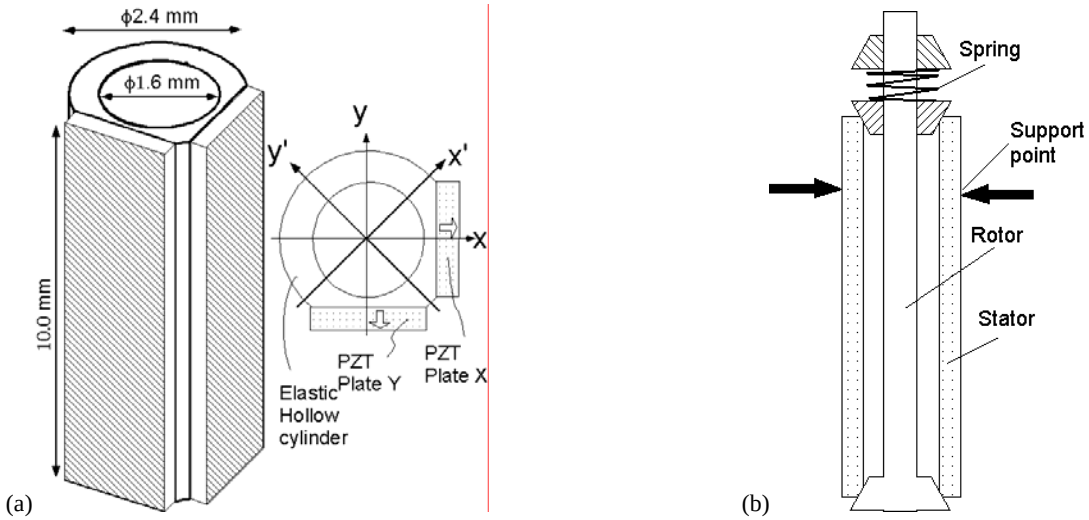

Figure 1: (a) Structure of the stator (b) Assembly of the motor.

The outside surface of a hollow metal cylinder was flattened on two sides at 90-degrees to each other and two uniformly electroded rectangular piezoelectric plates were bonded onto these two flattened surfaces (Fig. 1(a)). The basic configuration of the motor is shown in Fig. 1(b). Since the stator is symmetric with respect to the x'-axis, the area moment of inertia about the principal axis is on the x'-axis. The area moment of inertia about the other principal axis is on the y'-axis. This causes the stator to have two degenerated orthogonal bending modes, whose resonance frequencies are close to each other. The split of the bending mode frequencies is due to the partially square/partially circular outside surface of the hollow cylinder. The orthogonal bending modes correspond to the minimum and maximum bending moment of inertia of the beam (stator). Since the piezoelectric plates are oriented by 45^{o} to the direction of minimum and maximum bending moment of inertia, driving one piezoelectric plate (while short circuiting the other to ground) at a frequency between the two orthogonal bending mode frequencies excites both modes, thus, causing the cylinder to wobble. When the other piezoelectric plate is driven at the same frequency, the direction of wobble motion is reversed. The assembled motor is shown in Fig. 2.

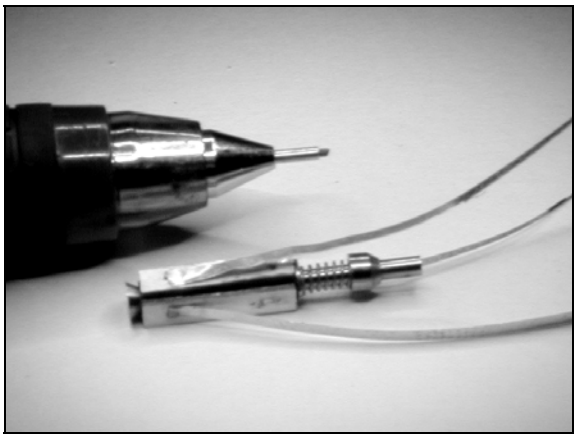

Figure 2: Photo of the assembled motor.

3. FINITE ELEMENT ANALYSIS AND OPTIMIZATION

The behavior of the free stator was simulated using ATILA [11] finite element. Tailoring dimensions of the metal and piezoelectric ceramics equated the two orthogonal bending mode frequencies of the stator. The piezoelectric plates on the surface of the cylinder were placed in such a way that one piezoelectric plate can excite the two orthogonal bending modes of the stator. Fig. 3(a) shows the two orthogonal bending mode shapes when only the plate on the x-axis (plate X) was excited, while the electrode of the plate Y was short-circuited. Wobble motion was generated on the cylinder when only one piezoelectric plate is excited between the two orthogonal bending modes frequencies (Fig. 3(b)). When the other piezoelectric plate was excited at the same frequency, the direction of wobble motion was reversed.

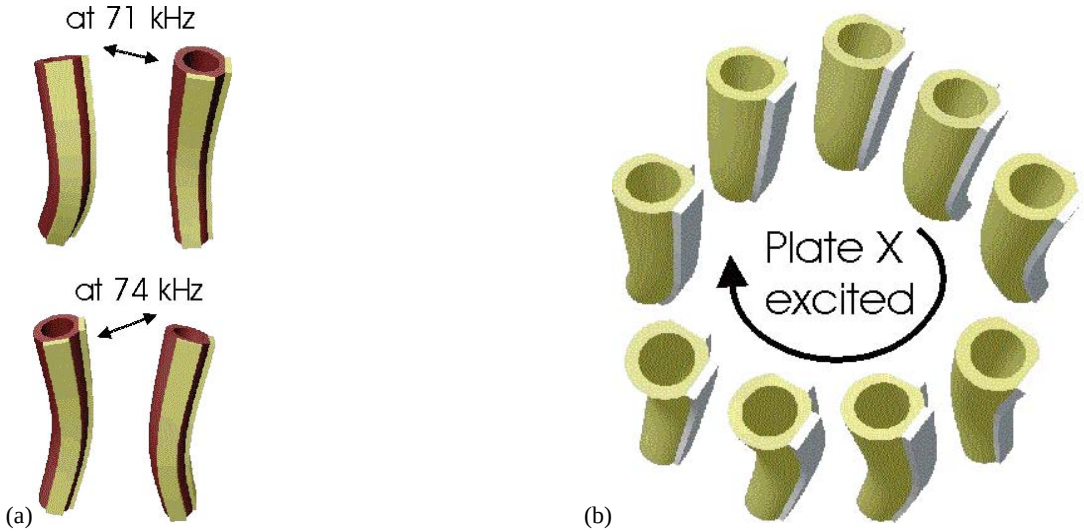

Figure 3: (a) Two orthogonal mode shapes (71 and 74kHz) when plate in x-axis is excited, (b) Wobble motion in clockwise direction can be generated on the cylinder when plate in x-axis is excited. When the other piezoelectric plate is excited at the same frequency, the direction of wobble motion can be reversed.

More recent work on this structure has focused on optimization using a combination of finite element analysis and genetic algorithm (FEA+GA).

Genetic algorithms presume that the potential solution of any problem is an individual and can be represented by a set of parameters. These parameters are regarded as the “genes” of a “chromosome,” which is a representation of the individual (Fig. 4). The chromosome can be structured and is often represented by a string of values in binary form. A positive value, generally known as a “fitness” value, is used to reflect the degree of “fitness” of the chromosome for the problem. Clearly, the fitness value is closely related to the objective value, which reflects how well an individual performs. Fig. 5 shows the design parameters selected for the tube-shaped motor as well as results from the finite element analysis carried out with ATILA.

Genetic algorthim terminology	**Example**	**Description and comments**
Genes	$P_1, P_2, ..., P_M$	Design parameters
Alleles	P_1 0, 1, 2, ..., 7 P_2 0, 1, 2, ..., 31 ⋮ ⋮ P_M 0, 1, 2, ...	Values taken by the parameters (length, thickness, radius, etc.)
	Binary representation 0 1 0 = P_1 = 2 0 0 1 1 0 = P_2 = 6 ⋮ ⋮ ⋮ 0 1 ··· 0 1 = P_M	
Chromosome or individual	A Tonpilz transducer	A solution described by the design parameters
Genotype	P_1 P_2 P_M 0 1 0 0 0 1 1 0 ··· 0 1 ··· 0 1	A binary string
Phenotype	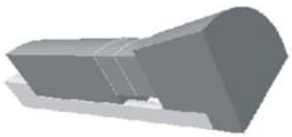	A possible design

Figure 4: Brief glossary of genetic algorithms terminology.

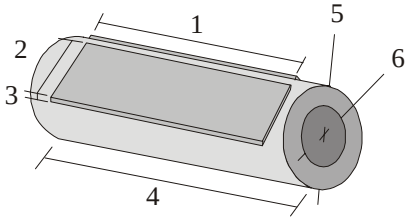

(a)

Piezoelectric elements:
1 - Length
2 - Width
3 - Thickness

Brass tube:
4 - Length
5 - Outer diameter
6 - Inner diameter

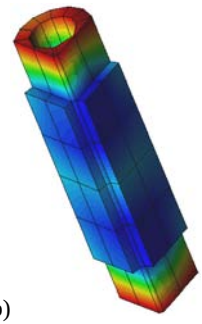

(b)

Figure 5: (a) Design parameters selected for the motor; (b) ATILA results.

Throughout a genetic evolution, the fitter chromosome has a tendency to yield good quality “offspring,” which means a better solution to the problem. A “population” pool of chromosomes has to be installed, and these can be randomly set initially. In each cycle of the genetic operation a subsequent “generation” is created from the chromosomes in the current population. Typically, this step involves three operators, “selection,” “crossover” and “mutation,” to direct the population towards convergence at the global optimum. The selection operator attempts to apply pressure upon the population in a manner similar to that of natural selection found in biological systems. Poorer performing individuals are weeded out and better performing, or fitter, individuals have a greater than average chance of promoting the information they contain within the next generation.

The crossover operator allows solutions to exchange information in a way similar to that used by a natural organism. The method consists of choosing pairs of individuals promoted by the selection operator, randomly selecting one or more points within the binary strings, and swapping the information (bits) from one point to another between the two individuals. The mutation operator is used to randomly change the value of single bits within individual strings. Excessive use of this operator may disrupt the evolution process.

The application of genetic algorithms to ultrasonic devices presents some difficulties. One of them concerns the coding of the genes, which may not always be regularly spaced integer numbers. For instance, design parameters usually correspond to the dimensions of the device. Eventually, these dimensions will be machined using traditional machine-shop techniques, and will be subject to constraints such as the size availability of the raw materials and the tolerance limits of the machining equipment. Therefore, most problems require that design parameters be real numbers, and often, discrete values. Discrete values can easily be mapped into a lookup table that the algorithm can consult to code and decode the corresponding gene. A simple and efficient solution for real values consists of considering a tolerance on the parameter value.

A genetic algorithm code following the general rules described above has been programmed in object-oriented Pascal on a PC platform, and tested on several structures [12]. The connection between GA and FEA takes place as illustrated in Fig. 6. The general flow diagram is similar to that of the genetic algorithm itself, except for the evaluation function, which is now more complex and includes the finite element analysis.

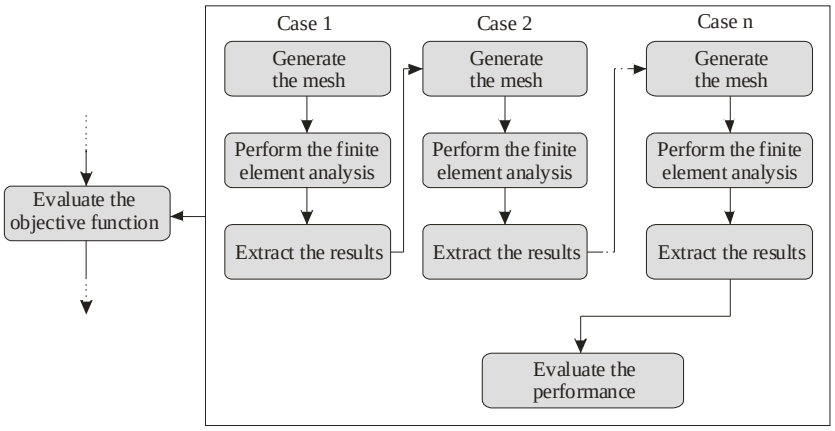

Figure 6: The combination of the FEA and GA methods takes place at the level of the evaluation function.

It is important to emphasize at this point that the evaluation function may include more than a single finite element run. Indeed, to evaluate the performance of the stator of an ultrasonic motor, it is required to determine, in general, the resonance frequency of each participating mode, its electromechanical coupling factor, and the resulting motion produced at the contact interface. Usually, one or two modal analyses are required to determine the characteristics of the modes, and a harmonic analysis is necessary to determine the shape of the ellipse.

There is, therefore, more than one call to the finite element program (ATILA) for the evaluation of each individual. This increases the order of the algorithm rather significantly and may result in long computation times. To alleviate this problem, great care should be taken in minimizing the size and complexity of each finite element mesh. As a result, each finite element case may use a different mesh that enhances the computation time for that run.

Finally, the genetic algorithm provides some advantages with respect to parallel computation. It is clear that the evaluation of each individual, for instance, can take place independent of the other individuals. Therefore, on a multiprocessor environment, it is possible to evaluate two or more individuals in parallel. This parallelization feature was incorporated in our program.

The program that was developed to implement the technique presented above is rather general. The genetic algorithm itself does not require modifications from one problem to another. Only the general settings (population size, gene size, probabilities of crossover and mutation) can be modified depending on the problem at hand. The finite element mesh (or meshes) is, of course, problem dependent. However, using meta-functions (that we also developed) for the creation of the mesh makes it relatively easy to generate a mesh for any given problem, whether two- or three-dimensional.

Finally, the most sensitive part that must be modified for every problem is the function that evaluates the performance of each individual based on the finite element results obtained. Even for one given problem, this function may also depend on the type of result that is sought. Usually, this evaluation function will contain terms associated with the operating frequency of the stator, the electromechanical coupling factor associated with each participating mode, and the elliptical factor associated with the vibration. Other terms, such as stresses, mass, volume, etc. can also be added.

(a)

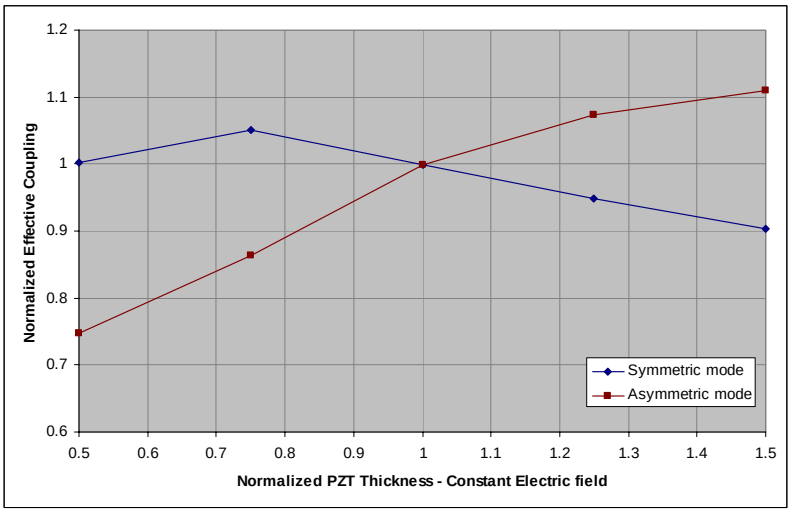

(b)

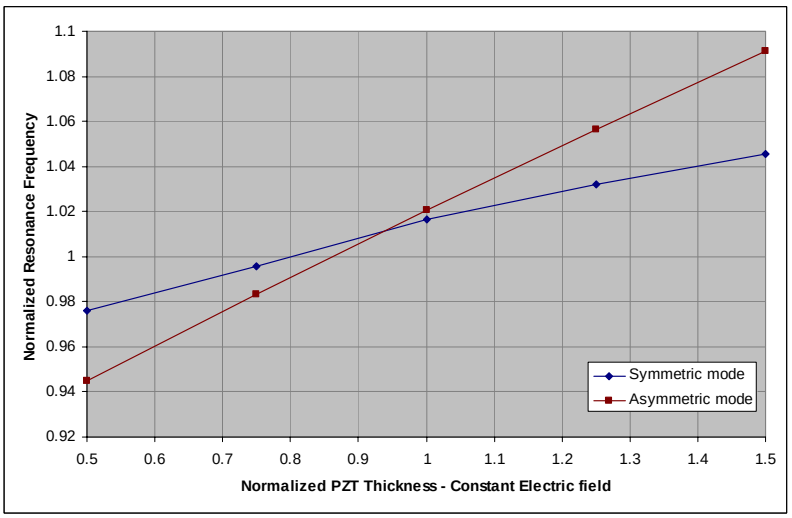

Figure 7: Results obtained from the FEA+GA procedure: (a) Effective coupling; (b) Resonance frequency. Symmetric and Asymmetric refer to the two bending modes of the tube structure.

In the case of this study, the FEA+GA procedure was aimed at determining the values of the design parameters that optimize the effective coupling coefficient as well as the frequencies of the two bending modes. For instance, in Fig. 7 are shown two examples obtained from the optimization procedure. As a function of the thickness of the piezoelectric elements, the effective coupling coefficient of the two modes can be adjusted. The same remark goes for the resonance frequencies of the modes. Finally, similar results could be reported for all the other design parameters.

A small version of the tube motor has been tested [13] and the results are summarized in the next section. The optimization work is currently in progress and addresses a variety of other structures. Results for these structures will be reported in future papers.

4. ASSEMBLING THE MOTOR

The stator of the prototype motor consists of a hollow metal tube (brass) with an outer diameter of 2.4 mm, an inner diameter of 1.6 mm, a length of 10 mm and two rectangular piezoelectric plates with dimensions, 10 mm in length, 2 mm in width and 0.5 mm in thickness. The outside surface of the metal cylinder was ground on two sides at 90-degrees to each other to obtain two orthogonal flat surfaces. The distance from the flat surface to the center of the tube was 1.0 mm. The PZT plates (APC841, APC International Ltd.), which were electroded uniformly and poled in the thickness direction, were bonded onto the flat orthogonal surfaces of the cylinder using an epoxy and cured at 60^0C. The rotor was a cylindrical rod and it was pressed by a spring, by approximately 0.72 N pre-stress, using a pair of stainless steel ferrules.

As a first step to clarify the behavior of the stator, the admittance spectra of the free stator were measured. Fig. 8(a) and 8(b) show the magnitude and phase of the free stator when plate X or Y was excited. When plate X was excited while short-circuiting the electrode of plate Y to the ground, the stator had two degenerated bending mode resonance frequencies around 71.8 and 74.0 kHz. When plate Y was excited, the stator showed a similar behavior.

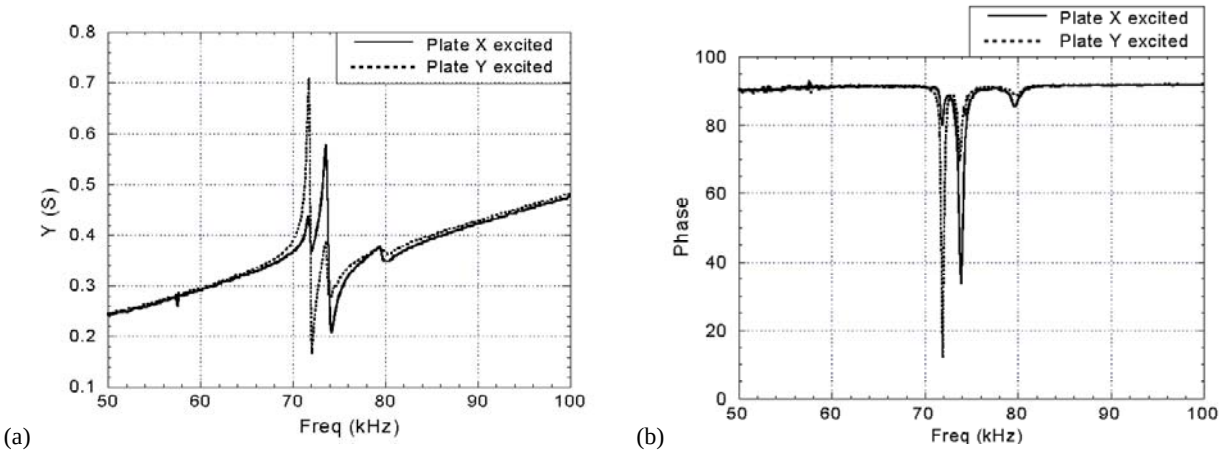

Figure 8: (a) Magnitude of admittance spectrum of the free stator when plate X or Y was excited, (b) Phase of the admittance spectrum of the free stator when plate X or Y was excited.

The peak-to-peak displacement spectrum around the two orthogonal bending mode frequencies in the x and y-axes directions was also measured. A function generator (HP33120A) and a power amplifier (NF4010) were used to excite the stator. By exciting either plate X or plate Y, the vibration velocity in x and y-axes directions was measured with two Laser Fiber Optic Interferometers (Politec OFV-3001/OFV-311). The displacement spectrum in the x and y directions when only plate X was excited is shown in Fig. 9(a). When only plate Y was excited, similar behavior was obtained and it is shown in Fig. 9(b).

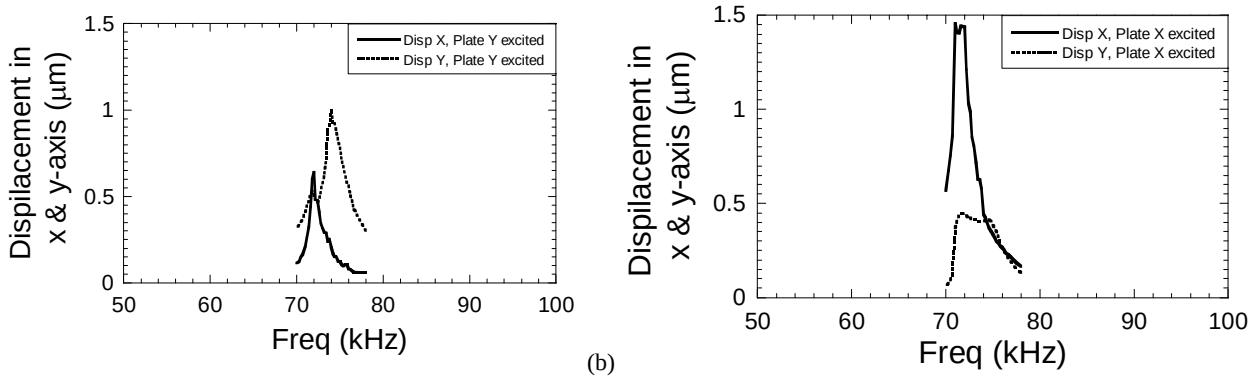

Figure 9: Amplitude of the displacement in x and y directions around two orthogonal resonance frequencies, (a) when plate X was excited, (b) when plate Y was excited.

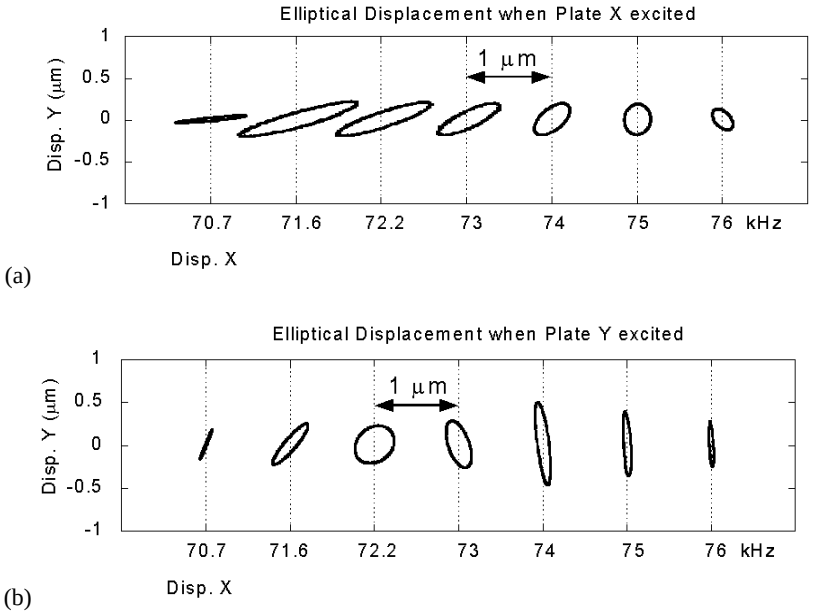

Figure 10: Elliptical displacements at frequencies 70.7, 71.6, 72.2, 73, 74, 75 and 76 kHz (a) when plate X was excited and, (b) when plate Y was excited. The direction of wobble motion is clockwise and counterclockwise, respectively.

The wobble motion in the xy-plane was also verified by measuring the magnitude of the vibration velocity in x and y directions at the same time. First, plate X was excited at frequencies of 70.7, 71.6, 72.2, 73, 74, 75, 76 kHz, with an input voltage of 112.0 V p-to-p. The elliptical displacements in x and y directions were then calculated using the vibration velocity data. The results are plotted in Fig. 10(a). The measurements were repeated by exciting only plate Y and the results are shown in Fig. 10(b). The interesting points here are: i) the direction of wobble motion when only plate X was excited was clockwise, and counterclockwise when only plate Y was excited, ii) the wobble motion, when only plate X was excited, was almost identical to the wobble motion when only plate Y was excited at the same frequency. In conclusion, the designed motor can be driven with a single AC source and exciting either plate X or Y, the direction of the rotation can be reversed.

5. MOTOR CHARACTERISTICS

The performance of the motor was measured using a transient characterization method, which was initially proposed by Nakamura [14]. The principle of this method is mounting a load (usually a disk whose moment of inertia is known) onto the motor, running the motor, and, finally, analyzing the transient speed obtained as a function of time. More explicitly, the angular acceleration of the motor is calculated from the speed measurement by Newton's second law. The transient torque is then calculated by multiplying the angular acceleration with the moment of inertia of the load. Using this method, the starting transient response of the motor gives the speed-torque relation. Similarly, the friction coefficient between the rotor and the stator can be estimated from the transient response for stopping the motor.

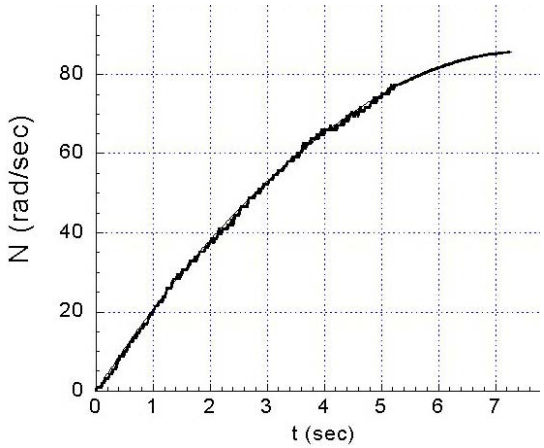

Figure 11: Transient response of the motor at 120 V.

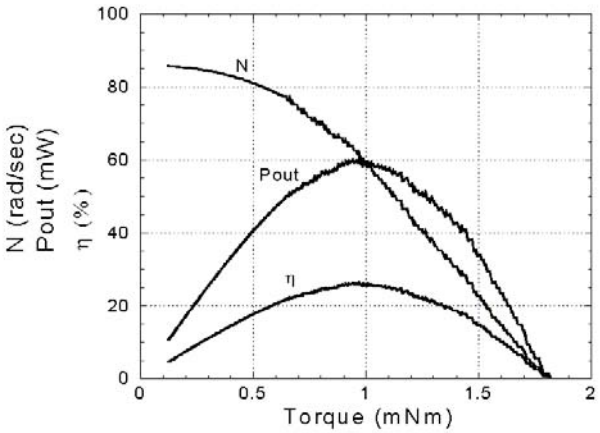

Figure 12: Load characteristics of the motor.

The load, a metal disk (60g) with a diameter of 34mm and moment of inertia (8.6kg·mm^2) was mounted onto the stator. The motor was then driven with an AC voltage of 120 V at 69.5 kHz. The position of the rotating disk was detected through an optical encoder (US Digital HEDS-9100-S00). The transient position data were then converted into voltage signal using a frequency-to-voltage converter.

Since the output voltage of the converter is proportional to the input frequency, the speed of the motor was obtained with a simple gain factor. The transient speed of the motor under loaded condition is shown in Fig. 11 when plate X is excited. The angular acceleration of the motor was estimated using the derivative of the angular speed. Finally, the transient torque was calculated by multiplying the angular acceleration with the moment of inertia of the rotating disk. The steady state speed reached 86 rad/sec in 7 sec. The load characteristics of the motor were obtained by plotting the transient speed as a function of transient torque (Fig. 12). Same results were obtained when plate Y was excited.

A starting torque of 1.8 mNm at 120 Volt is similar to other bulk piezoelectric cylindrical type micro motors in literature and almost one order of magnitude higher than that of a thin film motor with a similar size [15,16,17]. The product of output torque with output speed gives the output power. A maximum power of 60 mW was obtained at a speed of 60 rad/sec and a torque of 1 mNm. The efficiency curve that was obtained by dividing the output mechanical power to input electrical power is also shown in Fig. 9. It is directly proportional to the product of torque and angular velocity and inversely proportional to the input power, which is the product of voltage and current waveforms. The maximum efficiency of 25 % at 120 V is similar to other bulk cylindrical type micro piezoelectric motor [17].

6. CONCLUSION

This paper presented the design of a new Multi-Mode-Single-Vibrator type piezoelectric motor. The rotation of this motor takes place by exciting two orthogonal bending modes of a hollow cylinder. We also showed how the finite element analysis and genetic algorithm (FEA+GA) procedure could be used to design the motor to specific operarting conditions.

The structure of the stator was analyzed by using the ATILA finite element code, and its dynamic behavior was predicted. The motor in this paper provided the following motor characteristics: torque, 1.8 mNm, speed, 60 rad/sec, power, 60 mW and efficiency, 25%.

Significant advantages of our metal tube motors to the PZT tube motors [18] are; (1) lower manufacturing cost, (2) simpler driving circuit (only one sine wave), and (3) higher scalability.

REFERENCES

[1] H. Flemmer, B. Eriksson and J. Wikander, "Control design and stability analysis of a surgical teleoperator," *Mechatronics*, vol. 9, iss.7, pp. 843-866, Oct. 1999.

[2] J. Tsujino, M. Takeuchi and H. Koshisako, "Ultrasonic rotary motor using a longitudinal-torsional vibration converter," in *IEEE Ultrasonics Symposium*, 1992, vol. 2, pp. 887-892.

[3] O. Ohnishi, O. Myohga, T. Uchikawa, M.Tamegai, T. Inoue and S. Takahashi, "Piezoelectric ultrasonic motor using Longitudinal-Torsional composite Resonance Vibrator," *IEEE Trans. Ultrason., Ferroelect., Freq. Contr.*, vol. 40, pp. 687-693, Nov. 1993.

[4] B. Koc, A. Dogan, Y. Xu, R.E. Newnham and K. Uchino, "An ultrasonic motor using a metal-ceramic composite actuator generating torsional displacement," *Jpn. J. Appl. Phys.* vol. 37, part 1, no.10, pp. 5659-5662, Oct. 1998.

[5] R. Le Letty, F. Claeyssen, F. Barillot, M. F. Six, P. Bouchilloux, "New Linear Piezomotors for High Force/Precise Positioning Applications," 1998 IEEE Industry Applications Conference, Thirty-Third IAS Annual Meeting, vol.**1**, pp. 213-217, October 1998.

[6] Y. Tomikawa, T. Takano, and H. Umeda, "Thin rotary and linear ultrasonic motors using double-mode piezoelectric vibrator of the first longitudinal and second bending modes," *Jpn. J. Appl. Phys.*, vol. 31, pp.3073-3076, Sept.1992.

[7] W. Williams and W.J. Brown, "Piezoelectric Motor," U.S. Patent 2439499, April 13, 1948.

[8] S. Ueha and Y. Tomikawa, *Ultrasonic Motors: Theory and Applications.* Oxford U.K.: Clarendon, 1993, pp.4-6.

[9] T. Sashida and T. Kenjo, *An Introduction to Ultrasonic Motors.* Oxford, U.K.: Clarendon, 1993, pp.6-8.

[10] J. Wallaschek, "Contact mechanics of piezoelectric ultrasonic motors," *Smart Mater. Struct.*, vol. 7, pp. 369-381, June 1998.

[11] ATILA User's Manual, Magsoft Corporation.

[12] P. Bouchilloux, Modeling and Testing of Ultrasonic Motors, Doctoral Thesis, Rensselear Polytechnic Institute, December 2001.

[13] B. Koc, S. Cagatay, and K. Uchino, "A Piezoelectric Motor Using Two Orthogonal Bending Modes of a Hollow Cylinder," *IEEE Trans. Ultrason., Ferroelect., Freq. Contr.*, vol. 49, pp. 495-500, Apr. 2002.

[14] K. Nakamura, M. Kurosawa, H. Kurebayashi, and S Ueha, " An Estimation of load characteristics of an ultrasonic motor by measuring transient response," *IEEE Trans. Ultrason., Ferroelect., Freq. Contr.*, vol. 38, pp. 481-485, Sep. 1991.

[15] M. Kurosawa, T. Morita and T. Higuchi, "A cylindrical ultrasonic micro motor based on PZT thin film," in *IEEE Ultrasonics Symposium*, 1994, vol.1, pp.549-552.

[16] T. Morita, M. Kurosawa and T. Higuchi, " A cylindrical micro ultrasonic motor using PZT thin film deposited by single process hydrothermal method," *IEEE Trans. Ultrason., Ferroelect., Freq. Contr.*, vol. 40, pp. 687-693, Nov. 1993.

[17] T. Morita, M. Kurosawa and T. Higuchi, " Cylindrical micro ultrasonic motor utilizing bulk Lead Zirconate Titanate (PZT)," *Jpn. J. Appl. Phys.*, vol. 38, pp.3347-3350, May1999.

[18] S.Dong, S.P.Lim, K.H.Lee, J.Zhang, L.C.Lim and K.Uchino, "Piezoelectric Ultrasonic Micromotors with 1.5 mm Diameter," *IEEE Trans. Ultrason., Ferroelect., Freq. Contr.*, to be published.